Chinese Chemical Letters 37 (2026) 112343

Contents lists available at ScienceDirect

Chinese Chemical Letters

journal homepage: www.elsevier.com/locate/cclet

Degradation mechanisms of bisphenol A in oxalic acid/Fe(III)/sodium percarbonate system: The key roles of iron oxalate complexes

Zhimin Xu[a,b], Siyu He[c], Lingzhi Wang[d], Lei Wen[a], Fangfang Li[b], Hongbo Peng[a,b,*], Siyao Wang[b], Kexin Chang[a], Bo Pan[b], Peng Gao[e,*]

[a] Faculty of Modern Agricultural Engineering, Kunming University of Science & Technology, Kunming 650500, China
[b] Yunnan Provincial Key Laboratory of Soil Carbon Sequestration and Pollution Control, Faculty of Environmental Science & Engineering, Kunming University of Science & Technology, Kunming 650500, China
[c] Food Science & Engineering, Kunming University of Science and Technology, Kunming 650500, China
[d] Institute of Traffic Engineering, Kunming University of Science and Technology, Kunming 650500, China
[e] City College, Kunming University of Science & Technology, Kunming 650500, China

ARTICLE INFO

Article history:
Received 14 July 2025
Revised 8 December 2025
Accepted 29 December 2025
Available online 30 December 2025

Keywords:
Sodium percarbonate activation
Organic acid
Fe(II)/Fe(III) cycle
Reactive oxygen species
Organic pollutants removal

ABSTRACT

Oxalic acid (OA) promotes the production of reactive oxygen species (ROS) and the degradation of pollutants, while it also enhances the reduction of trivalent iron (Fe(III)) in homogeneous Fenton systems. However, due to the coexistence of Fe(II) and OA-Fe(III)/hydroperoxide complex, the generation pathways of ROS and degradation mechanisms of pollutants have not been clarified. In this work, bisphenol A (BPA) was selected and its degradation mechanisms in the OA/Fe(III)/sodium percarbonate (SPC) system were investigated. Results showed that 99% of BPA degradation in OA/Fe(III)/SPC system, which was higher than that of single Fe(III) and SPC system (degradation ratio < 10%). OA promoted the formation of carbonate radicals ($CO_3^{\bullet-}$) and hydroxyl radicals ($^{\bullet}OH$). There was no remarkable relationship between the degradation ratio of BPA and the change of Fe(II) concentration, suggesting that the reduction properties of OA was not the direct cause of BPA degradation. By further analysis, the chelation of Fe(III) and OA resulted in an enormous potential difference between Fe(II) and Fe(III)-OA complex, which was more favorable for accepting electrons from Fe(II) intermediate, and forming more reactive ferrous complexes; moreover, iron oxalate ($Fe_2(C_2O_4)_3$) enhanced BPA degradation in the Fe(II)/SPC system, which also evidenced the above findings. Under neutral conditions (pH 7.0), peroxy intermediate (OA-Fe(III)-OOH) complex also contributed to $CO_3^{\bullet-}$/$^{\bullet}OH$ production and enhanced BPA degradation. These findings highlight the important role of OA in degradation of pollutants, which provides valuable insights for designing sustainable Fenton-based advanced oxidation processes.

© 2026 Published by Elsevier B.V. on behalf of Chinese Chemical Society and Institute of Materia Medica, Chinese Academy of Medical Sciences.

The escalating human activities have markedly increased exposure risks of diverse environmental pollutants, particularly endocrine disrupting compounds (EDCs), *via* various environmental media [1,2]. Ubiquitous in the environment, these compounds possess significant ecological toxicity [3,4]. Even at trace concentrations (ng/L), EDCs can induce physiological damage, including endocrine disruption and reproductive toxicity in aquatic organisms. However, many prevalent EDCs, such as bisphenol A (BPA), sulfamethoxazole (SMX), and phenol (PN), exhibit high environmental persistence, resisting complete natural degradation and gradually accumulating in ecosystems[5,6]. Hence, developing efficient removal technologies for EDCs like BPA is critical to mitigate environmental concerns.

As an ideal alternative of hydrogen peroxide (H_2O_2) in Fenton system when treating EDCs containing wastewater, sodium percarbonate (SPC, $Na_2CO_3 \cdot 1.5H_2O$) has several advantages: (1) Unlike liquid H_2O_2, which maintains relatively stable chemical properties below 40 °C, solid SPC presents pronounced susceptibility to photolytic and pyrolytic degradation under environmental conditions. SPC's stability can be further enhanced when encapsulated within protective matrices [7]; (2) SPC systems provide a wider range of reactive oxygen species (ROS), such as hydroxyl radicals ($^{\bullet}OH$), superoxide radicals ($O_2^{\bullet-}$), carbonate radicals ($CO_3^{\bullet-}$), and singlet oxygen, versatile for treating complex pollutants in industrial wastewater [8]; (3) The price of SPC ($300–350/t) is much cheaper than

* Corresponding authors.
E-mail addresses: mzxb817@163.com (H. Peng), Gpeng8205@163.com (P. Gao).

https://doi.org/10.1016/j.cclet.2025.112343
1001-8417/© 2026 Published by Elsevier B.V. on behalf of Chinese Chemical Society and Institute of Materia Medica, Chinese Academy of Medical Sciences.

that of H_2O_2 ($1000–1200/t) [9]. Therefore, SPC is receiving more attention in the removal of EDCs pollutants.

Various metals ions, including Fe(II), Cu(II), Zn(II), Mn(II), and Ni(II), along with their mineral-derived catalysts, have been shown to serve as effective catalysts in Fenton-based process [10–13]. Among these, iron-based catalysts are particularly notable due to their low cost, ease of operation, and environmental compatibility. Accordingly, a range of iron-based materials including zero-valent iron, iron oxides, iron minerals, and iron-containing composites, have been widely utilized to activate SPC for the degradation of EDCs. Nevertheless, despite being a green and efficient catalyst for SPC in Fenton-like systems, Fe(II) is subject to two major limitations in practical applications: One is the formation of insoluble iron sludge at neutral pH values, and the coexisting carbonates raise the difficulty of regulating pH at target acidic range (*e.g.*, 3.0–5.0); The other attributes to a slow regeneration rate of Fe(II) ($Fe(III) + H_2O_2 \rightarrow Fe(II) + H^+ + HO_2^{\bullet}$, at 25 °C) [14–16]. Therefore, achieving a stable activation of SPC and an efficient generation of ROS at the neutral pH range remains a great challenge.

Small-molecular-weight organic acids (SMOAs), such as malic acid (MA), tartaric acid (TA), oxalic acid (OA), citric acid (CA), gallic acid (GC), and protocatechuic acid (PC), are ubiquitously distributed in environmental matrices, originating from plant residues, root exudates, microbial metabolites, and the decomposition of organic pollutants [17,18]. SMOAs bear pronounced chelation and reduction capacities, making them ideal accelerators for efficient iron cycling in nature. Chelation and reduction can also benefit Fenton-like processes: In the reduction pathway, GC serves as a sacrificial reductant to regenerate Fe(II), which subsequently activates oxidants through electron transfer [19,20]. In the chelation pathway, protocatechuic acid (PC) forms a bidentate complex with Fe(III), which further modulates the electronic structure of Fe(III) and enhances the complex's reactivity with oxidants [21]. The SMOAs related peroxide intermediates (*e.g.*, PICA-FeIII-OOH in the presence of PC and Fe(III)) can also promote EDCs degradation or serve as precursors for ROS generation [14,22]. Hence, as bifunctional agents, SMOAs seem promising in activation of SPC and degradation of EDC pollutants. However, in Fenton-like systems, the introduction of SMOAs cannot avoid consumption of ROS and peroxides precursors. GC quenching $^{\bullet}OH$ by electron transfer has been found in previous study [20,23]. The impact of various organic acids on $^{\bullet}OH$ in Fenton-like system has been investigated, while limited information is available regarding $CO_3^{\bullet-}$ species since the introduction of SPC. In comparison to $^{\bullet}OH$, $CO_3^{\bullet-}$ prefers to react with electron-rich compounds containing N-/S-functional groups, aromatic compounds, and substituted phenolic moieties, and $CO_3^{\bullet-}$ maintains a steady-state concentration 100 to 1000 times higher than that of $^{\bullet}OH$ [24,25]. To this end, a thorough investigation is needed when introducing SMOAs into the SPC-based Fenton-like system, so as to reveal the mechanism beneath about the degradation of pollutants. In this research, oxalic acid (OA) was applied to treat BPA in the SPC/Fenton-like system, focusing on (1) the chelation and reduction properties of OA on SPC activation and BPA degradation; (2) the impact of Fe(III)/SPC dosage, solution pH, and OA characteristics on ROS generation and BPA degradation; (3) mechanisms and application principles of SMOA for BPA degradation in the Fe(III)/SPC system.

Mere degradation of BPA was observed in single OA, Fe(III), and SPC system (Fig. 1a), which may be due to the limited production of reactive species. However, the degradation ratio of BPA reached to 99.7 % within 60 min in the OA/Fe(III)/SPC system ($k_{obs} = 0.0854\ min^{-1}$). As the concentration of OA increased from 0 μmol/L to 50 μmol/L (Fig. 1b), the degradation ratio of BPA gradually increased from 8.4 % to 99.7 %, indicating that OA greatly enhanced the oxidation capacity of Fe(III)/SPC. However, the degradation ratio decreased to 90.4 % when the OA was raised to 70 μmol/L, which may result from the quenching of ROS by excessive OA. The function of Fe(III) was also crucial in the system: With the concentration increased from 0 to 100 μmol/L, the degradation ratio of BPA increased from 5.2 % to 99.7 %, and this value kept unchanged when continuously raising the Fe(III)'s concentration (Fig. 1c). In addition, the degradation ratio of BPA was gradually enhanced with the increase of SPC up to 200 μmol/L, followed by severe inhibition when SPC was at 300 μmol/L (Fig. 1d). As for the impact of initial pH, >99 % of BPA had been degraded within 60 min under the pH 3.0–7.0, indicating that acidic and neutral pH were both preferable for this process, while the degradation rate was in the order of pH 5.0 ($k_{obs} = 0.132\ min^{-1}$) > pH 3.0 ($k_{obs} = 0.106\ min^{-1}$) > pH 7.0 ($k_{obs} = 0.077\ min^{-1}$) > pH 9.0 ($k_{obs} = 0.022\ min^{-1}$) > pH 11.0 ($k_{obs} = 0.005\ min^{-1}$) (Fig. 1e). In addition to BPA, PN, SMX, TMX, and NB were also effectively removed within 1 h in the OA/Fe(III)/SPC system (Fig. 1f), proving the wide application range of OA/Fe(III)/SPC system.

In order to elucidate the degradation mechanisms of BPA in the OA/Fe(III)/SPC system, the reactive species were identified by scavenging experiments. Estimations of the quenching efficiency for different quenchers are detailed in Text S1 (Supporting information). Results showed that both TBA (scavenging over 95 % of $^{\bullet}OH$ but only 1 % of $CO_3^{\bullet-}$) and phenol (scavenging 95 % of $CO_3^{\bullet-}$ and $^{\bullet}OH$) significantly inhibited the degradation of BPA (Fig. 2a). Considering that $^{\bullet}OH$ readily acted as a precursor of $CO_3^{\bullet-}$ [8], it could be inferred that both $CO_3^{\bullet-}$ and $^{\bullet}OH$ were involved in the degradation process of BPA in the OA/Fe(III)/SPC system. Moreover, excess chloroform (scavenging over 95 % of $O_2^{\bullet-}$) nor N_2 purging had no impact on the degradation of BPA (Fig. 2b and Fig. S1 in Supporting information), thereby excluding the involvement of $O_2^{\bullet-}$ in this process. Furfuryl alcohol (FFA) fails to quench $^1O_2$ in the existence of $^{\bullet}OH$, while researchers have reported that the lifetime of $^1O_2$ in deuteroxide (D_2O) (68 ± 1 μs) was longer than that in H_2O (3.7 ± 0.4 μs) [26,27]. In current research, the BPA degradation followed the similar trend in both D_2O and H_2O, proving an insignificant role played by $^1O_2$ (Fig. 2b). Previous studies have reported the formation of carbon-centered free radicals in OA-assisted systems, *via* reactions such as ($^{\bullet}OH + C_2O_4^{2-} \rightarrow CO_2^{\bullet-} + CO_2 + H_2O_2$) [28]. However, given the strong nucleophilic character of $CO_2^{\bullet-}$ and its highly negative reduction potential ($E_0 = -2.2$ V), this species was more likely to participate in reduction reactions rather than directly attacking electrophilic compounds such as phenolic contaminants [29,30]. As illustrated in Fig. 1f, the efficient degradation of electrophilic substrates including BPA, PN, and SMX strongly suggested that $CO_2^{\bullet-}$ was not the primary ROS responsible for their oxidation.

To further investigate the contribution of ROS for the degradation of BPA in the OA/Fe(III)/SPC system, EPR tests were performed for different systems using 5,5-dimethyl-1-pyrroline *N*-oxide (DMPO) as a spin trap [31]. Obvious signals of DMPO-$^{\bullet}OH$ and DMPO–$CO_3^{\bullet-}$ were observed, demonstrating the generation of $^{\bullet}OH$ and $CO_3^{\bullet-}$ (Fig. 2c) [32]. The signals of $^{\bullet}OH$ and $CO_3^{\bullet-}$ in the OA/Fe(III)/SPC system were significantly higher than those in single Fe(III) and SPC systems, suggesting that OA could promote their production. Meanwhile, enhanced DMPO–$O_2^{\bullet-}$ (methanol as reaction solvent) and TEMP-$^1O_2$ signals were also observed in OA/Fe(III)/SPC system when compared with single SPC, OA/SPC and Fe(III)/SPC systems (Figs. 2d and e). Hence, OA, Fe(III), and SPC could produce ROS synergistically in the OA/Fe(III)/SPC system. However, the contribution of $O_2^{\bullet-}$ and $^1O_2$ to BPA degradation was limited, which might be due to the reaction specificity. A lower amount of $PMSO_2$ was detected when adding PMSO into the OA/Fe(III)/SPC system ($\eta[PMSO_2] < 5$ %, the molar ratio of $PMSO_2$ production to PMSO depletion), which demonstrated that the generation of Fe(IV) was rare and not primarily responsible for BPA degradation (Fig. 2f) [22]. In conclusion, $^{\bullet}OH$, $CO_3^{\bullet-}$ were dominant

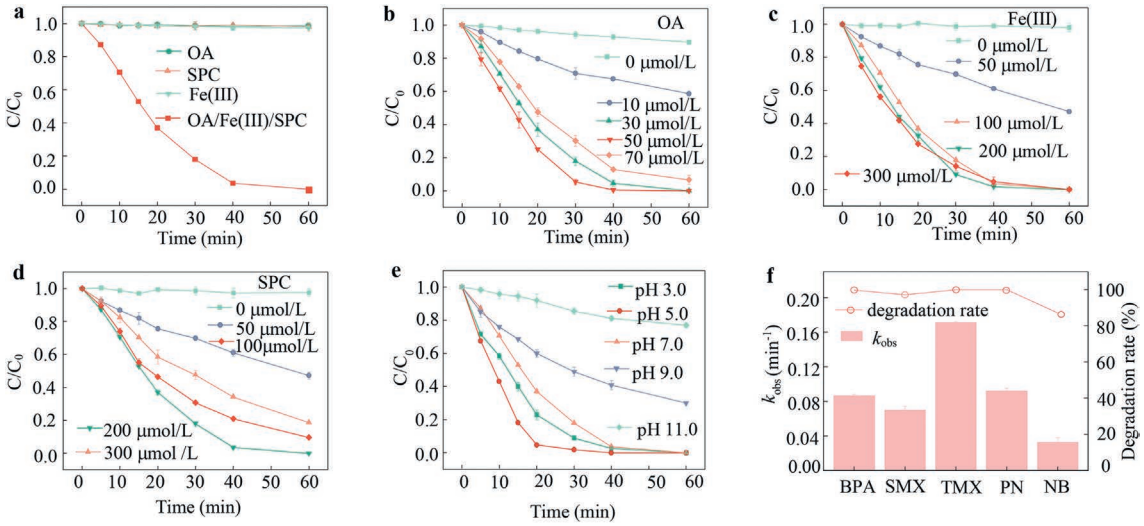


Fig. 1. Degradation ratio of BPA in the different systems (a), effect of OA concentration (b), Fe(III) concentration (c), SPC concentration (d), and initial pH (e) on BPA degradation, and (f) the calculated reaction rate constant (k_{obs}) of different pollutants in OA/Fe(III)/SPC system with [Fe(III)] = 100 μmol/L, [SPC] = 200 μmol/L, [pollutants] = 4.4 μmol/L, [OA] = 30 μmol/L (f), and pH 7.0.

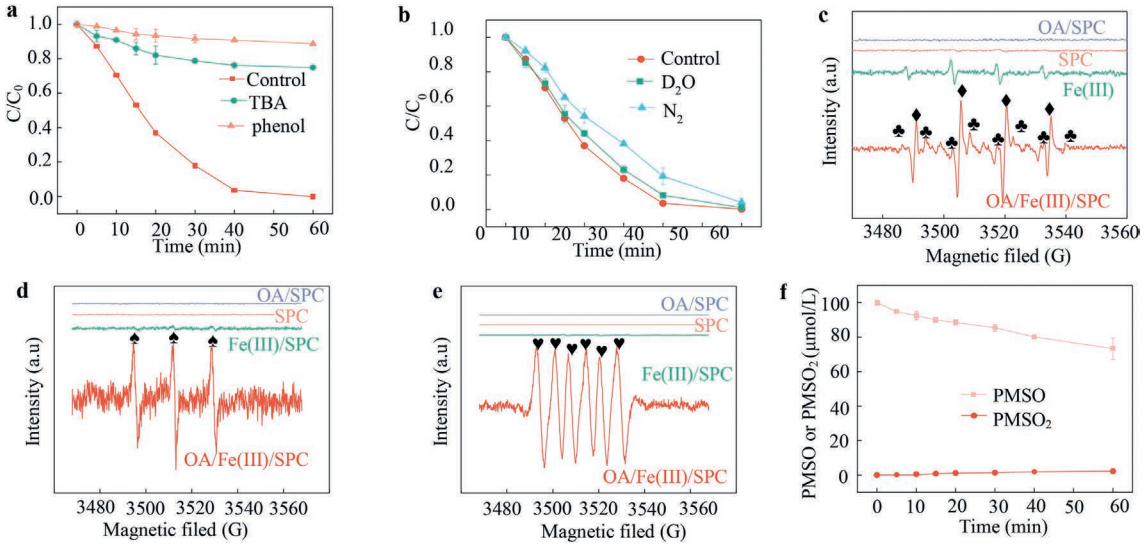


Fig. 2. (a) $^{\bullet}OH$ and $CO_3^{\bullet-}$ quencher effects on BPA degradation in OA/Fe(III)/SPC system. (b) Degradation of BPA in OA/Fe(III)/SPC system under N_2 and D_2O conditions. (c) EPR spectra of DMPO-$^{\bullet}OH$ (♦) and DMPO–$CO_3^{\bullet-}$ (♣) adducts. EPR spectra of DMPO–$O_2^{\bullet-}$ (♥) (d) and TEMP-$^1O_2$ (♠) (e) adducts. (f) PMSO depletion and $PMSO_2$ generation. Conditions: [Fe(III)] = 100 μmol/L, [SPC] = 200 μmol/L, [BPA] = 4.4 μmol/L, [OA] = 30 μmol/L.

reactive species and played a crucial role in the OA/Fe(III)/SPC system, while $O_2^{\bullet-}$, Fe(IV), and $^1O_2$ were limited in quantity and reactivity by contrast.

The formation of Fe(II) in the Fe(III)/SPC, OA/Fe(III) and OA/Fe(III)/SPC systems was investigated in the absence of BPA (Fig. 3a) was investigated to elucidate the role of OA in the Fe(III)/Fe(II) redox cycles. In the Fe(III)/SPC system, the production of Fe(II) was essentially negligible; By comparison, about 39.7 % Fe(III) were reduced to Fe(II) in the OA/Fe(III) system; The presence of SPC accelerated the consumption of Fe(II), while chloroform and N_2 (scavenging over 95 % of $O_2^{\bullet-}$) inhibited the production of Fe(II) in the OA/Fe(III)/SPC system (Fig. 3a), indicating that $HO_2^{\bullet}/O_2^{\bullet-}$ also promoted the reduction of Fe(III), and similar findings have also been reported elsewhere (Fe(III)-OA + $HO_2^{\bullet}/O_2^{\bullet-}$ → Fe(II)-OA + O_2 (H^+)) [20]. Therefore, OA benefited reduction of Fe(III) to Fe(II) *via* $^{\bullet}OH/O_2^{\bullet-}$ production and made up for the Fe(II) consumption by SPC.

To assess the impact of organic acid structure on Fe(II) production and BPA degradation in the OA/Fe(III)/SPC system, SMOAs with different functional groups were tested including acetic acid (AA), lactic acid (LA), malic acid (MA), tartaric acid (TA), oxalic acid (OA), and citric acid (CA). Previous studies have demonstrated that the removal efficiency of BPA was significantly higher in OA-Fenton-like processes than in systems utilizing other chelating agents, such as TA and CA [33]. The results showed that the concentration of Fe(II) continued to increase along with the degradation of BPA. Though there was difference in BPA degradation performance, the regeneration of Fe(II) was no longer the rate limiting step of Fenton reaction in the presence of SMOAs (Figs. 3b and c). It was noteworthy that the OA/Fe(III)/SPC system exhibited a higher H_2O_2 consumption rate than that of the Fe(II)/SPC system (Fig. S1b). The higher total Fe(II) concentration in the OA/Fe(III)/SPC system (compared to the Fe(II)/SPC system) further suggested the involvement of a non-reductive process mediated by OA. Therefore,

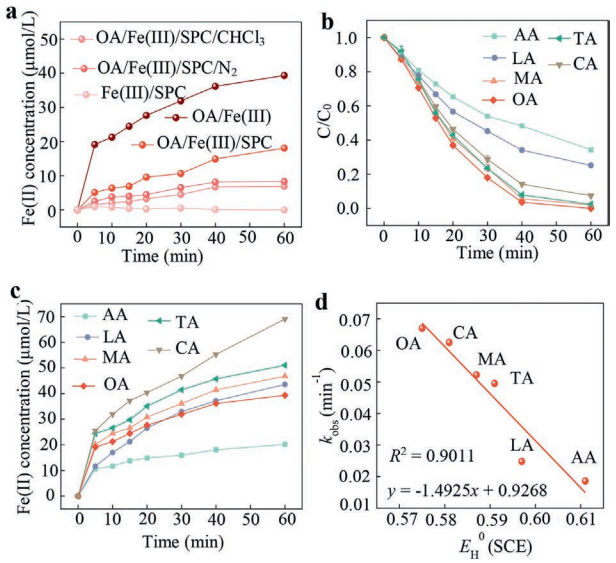


Fig. 3. (a) The generation of Fe(II) in different systems. Effect of different SMOAs on BPA degradation in the Fe(III)/SPC system (b) and Fe(II) generation (c). (d) Relationship between k_{obs} of BPA and redox potential ($E_H{}^0$ (SCE)) of organic acid-Fe(III)/Fe(II) complex. Conditions: [Fe(III)] = 100 μmol/L, [SPC] = 200 μmol/L, [BPA] = 4.4 μmol/L, [SMOA] = 30 μmol/L, $[pH]_0$ = 5.0.

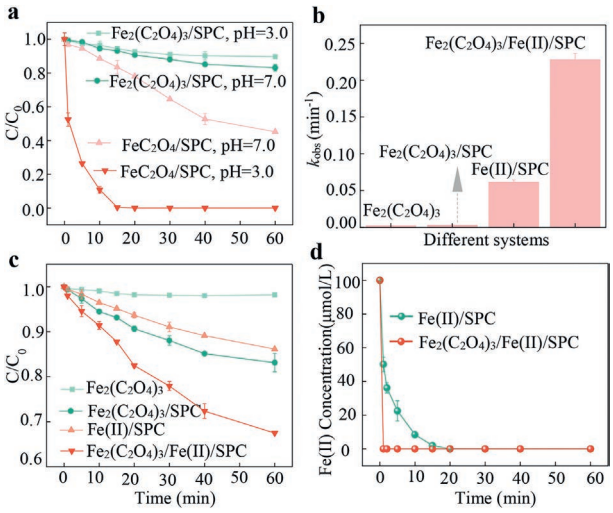


Fig. 4. (a) Effect of SPC for the degradation of BPA by $Fe_2(C_2O_4)$ and FeC_2O_4. (b) The values of k_{obs} by different systems under acid condition. Degradation of BPA by different systems under neutral conditions (c) and the exist of Fe(II) in different systems (d). Conditions: $[FeC_2O_4]/[Fe_2(C_2O_4)]/[Fe(II)]$ = 100 μmol/L, [SPC] = 200 μmol/L, [BPA] = 4.4 μmol/L, [OA] = 30 μmol/L.

there may be more than one pathway to generate $^{\bullet}OH$ and $CO_3^{\bullet-}$ in Fe(III)/SPC like systems driven by SMOAs.

By further analysis, a significant correlation was observed between k_{obs} of BPA and the redox potential of SMOAs-Fe(III)/Fe(II) complex (Fig. 3d). It should be emphasized that the redox potential serves as a critical indicator, reflecting not only the electron-donating/accepting capacity of a species but also, to a certain extent, the coordination capability of ligands. This correlation is substantiated by the observed relationship between redox potentials and the equilibrium constants of Fe(II)/Fe(III)-ligand complexation (Text S2 and Fig. S2 in Supporting information). Consequently, systematic investigation into reactive oxygen species (ROS) generation and pollutant degradation mechanisms during coordination processes is warranted.

The coordination ability of OA for BPA degradation was investigated using UV–vis spectroscopy. New absorption bands were observed at 260–350 nm and 280–580 nm in the OA/Fe(III) system under acidic and neutral conditions, respectively (Fig. S3 in Supporting information), which were related to complexes formed *via* chelation of OA and Fe(III) [34,35]. Studies have shown that the iron in the coordinated state was mainly in the form of iron oxalate $Fe_2(C_2O_4)_3$ and ferrous oxalate ($Fe(C_2O_4)$) at pH 3.0, while iron in the coordinated state exists mainly as FeC_2O_4, $Fe(C_2O_4)_2^{2-}$, and $Fe_2(C_2O_4)_3$ at pH 7.0 [35]. In order to further investigated the impact of OA-Fe(III) complex on SPC activation, $Fe_2(C_2O_4)$/SPC and FeC_2O_4/SPC systems were constructed. The pH of FeC_2O_4 and $Fe(C_2O_4)_2^{2-}$ was adjusted based on previous research [35]. The degradation ratio of BPA was 18.6% in $Fe_2(C_2O_4)_3$/SPC system at pH 7.0 (Fig. 4a), slightly higher than that of Fe(III)/SPC system (9.4%) (Fig. 1a). In contrast, the degradation ratio of BPA in the FeC_2O_4/SPC system was 100% and 49.4% under acidic and neutral conditions, respectively, both higher than that of the Fe(II)/SPC system (Fig. 4c), this suggested that the complexes formed by coordination complexation are more reactive.

Interestingly, the addition of SPC resulted in a significant hysteresis for the absorption peaks (neutral conditions only), and similar OA-Fe(III)-OOH complex was also observed when H_2O_2 was adopted [14,36]. And the intensity of OA-Fe(III)-OOH complex slightly decreased when 100 μg/L BPA were added, suggests its reaction with BPA (Fig. S4 in Supporting information). In order to further confirm the role of OA-Fe(III)-OOH complex for BPA degradation, $H_2PO_4^-$ ($\log K_{Fe(III)\text{-}H_2PO_4^-} = 3.5$) as the inorganic competing ligand was dosed [36]. $H_2PO_4^-$ was proved to significantly inhibit BPA degradation and lead to a decreased of $^{\bullet}OH$ (Fig. S5 in Supporting information). To sum up, in neutral conditions, OA-Fe(III)-OOH complex was beneficial to $^{\bullet}OH$ generation and BPA degradation.

It should be noted that under acidic conditions, a distinct adsorption peak was observed in the OA/Fe(III) system within the wavelength range from 260 nm to 350 nm, which implied the presence of coordinated iron species Moreover, Fe(III) as a hard Lewis acid, can form complexes with ligand with large stability constants. However, Fe(II) as a borderline Lewis acid binds less strongly to the ligand than Fe(III) [37]. Thus, Fe(II) and $Fe_2(C_2O_4)_3$ were the main forms of iron present under acidic conditions. The effects of Fe(II)/SPC and $Fe_2(C_2O_4)_3$/Fe(II)/SPC systems on BPA degradation were compared in acidic condition. The degradation rate of BPA in the $Fe_2(C_2O_4)_3$/Fe(II)/SPC system was 3.8 times higher than that of Fe(II)/SPC system, and this value was also higher than that in both single and binary systems (Fig. 4b). However, no similar enhancement phenomenon was observed under neutral conditions (Fig. 4c). In addition, the consumption rate of Fe(II) was higher in the $Fe_2(C_2O_4)_3$/Fe(II)/SPC system (Fig. 4d). Therefore, the effect of the coordination process was not negligible in the enhancement of the Fe(II)/SPC reaction process by $Fe_2(C_2O_4)_3$, in addition to the generation of more reactive ferrous complexes. Nevertheless, due to the complexity of the iron morphology in the OA/Fe(III)/SPC system, it is difficult to quantify the contribution of the $Fe_2(C_2O_4)_3$ generated to the enhancement of the Fe^{2+}/SPC process.

Based on kinetic and spectroscopic measurements, distinct catalytic mechanisms were identified under acidic *versus* neutral conditions. Under acidic conditions, the dominant pathway involved chelation between Fe(III) and OA, leading to a significant redox potential difference between the OA-Fe(III)-complex and Fe(II). This potential gap facilitated electron transfer from Fe(II), promoting the formation of a highly reactive ferrous complex. The reaction process during BPA degradation under acidic conditions initiated with the coordination and reduction of Fe(III) by OA, yielding Fe(II) and OA-Fe(III)/OA-Fe(II) complexes (Eqs. 1 and 2). Subsequent introduction of SPC triggered direct reactions with these iron complexes.

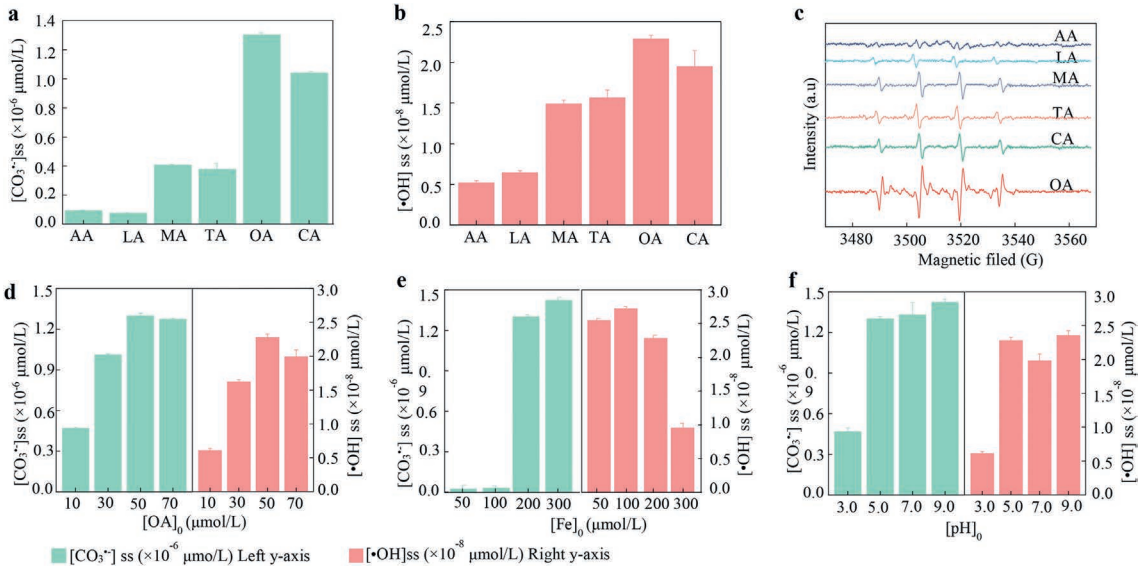


Fig. 5. Effect of different organic acids on the steady-state concentration of $CO_3^{\bullet-}$ (a) and $^{\bullet}OH$ (b). (c) EPR spectra for different organic acid systems. Effect of OA concentration (d), Fe(III) concentration (e), and pH (f) on the steady-state concentration of $^{\bullet}OH$ and $CO_3^{\bullet-}$. Conditions: [Fe(III)] = 100 μmol/L, [SPC] = 200 μmol/L, [BPA] = 4.4 μmol/L, [OA] = 30 μmol/L.

The OA-Fe(III) species accepted electrons from Fe(II) to form OA-Fe(II) complex, which further reacted with H_2O_2 to generate $^{\bullet}OH$ (Eqs. 3–5). In contrast, under neutral conditions, ROS generation was primarily governed by OA-driven coordination process. Specially, the OA-Fe(II) complex activated SPC to produce $^{\bullet}OH$, while a peroxyl intermediate complex (OA-Fe(III)-OOH) also contributed to $^{\bullet}OH$ formation (Eqs. 6 and 7).

$$\text{Fe(III)} + \text{OA} \rightarrow \text{OA-Fe(III)} \quad (1)$$

$$\text{Fe(III)} + \text{OA} \rightarrow \text{OA-Fe(II)} \quad (2)$$

$$\text{Fe(II)} + H_2O_2 \rightarrow \text{Fe(III)} + {}^{\bullet}OH + OH^- \quad (3)$$

$$\text{Fe(II)} + \text{OA-Fe(III)} \rightarrow \text{Fe(II)-OA} + \text{Fe(III)} \quad (4)$$

$$\text{Fe(II)-OA} + H_2O_2 \rightarrow \text{Fe(III)-OA} + {}^{\bullet}OH + OH^- \quad (5)$$

$$\text{OA-Fe(III)} + H_2O_2 \rightarrow \text{OA-Fe(III)-OOH} \quad (6)$$

$$\text{OA-Fe(III)-OOH} \rightarrow \text{Fe(II)} + \text{OA} + {}^{\bullet}OH \quad (7)$$

$$CO_3^{2-} + {}^{\bullet}OH \rightarrow CO_3^{\bullet-} + OH^- \quad (8)$$

$$HCO_3^- + {}^{\bullet}OH \rightarrow CO_3^{\bullet-} + H_2O \quad (9)$$

$$H_2O_2 + HCO_3^- \leftrightarrow HCO_4^- + H_2O \quad (10)$$

$$HCO_4^- \rightarrow CO_3^{\bullet-} + H^+ \quad (11)$$

Current research has extensively documented the effects of reductants on $^{\bullet}OH$, $SO_4^{\bullet-}$, and Fe(IV) [20,38], while the influence of reductants on $CO_3^{\bullet-}$ has received limited attention. To elucidate the differential contributions of ROS under varying operational conditions, the key parameters including solution pH, Fe(III) dosage, SPC concentration and SMOAs type-governing BPA degradation in the OA/Fe(III)/SPC system were investigated. The steady-state concentrations of $^{\bullet}OH$ and $CO_3^{\bullet-}$ were quantified through kinetic modeling, as described in Text S3 (Supporting information). The concentration of $^{\bullet}OH$ and $CO_3^{\bullet-}$ for different SMOAs at initial pH 7.0 was OA > CA > TA > MA > LA > AA (Figs. 5a and b), which was consistent with the results of EPR test (Fig. 5c). The steady-state concentration of $^{\bullet}OH$ and $CO_3^{\bullet-}$ increased and then decreased when the OA concentration increased, mainly due to the inhibiting effect of excess OA (Fig. 5d). The difference was that the inhibiting effect of 70 μmol/L OA on $CO_3^{\bullet-}$ was weak, suggesting that $CO_3^{\bullet-}$ displayed lower selectivity towards OA when compared to $^{\bullet}OH$. This finding also suggested that employing $CO_3^{\bullet-}$ for BPA degradation in OA/Fe(III)/SPC system could partially mitigated the adverse effects caused by excess OA. The steady-state concentrations of $^{\bullet}OH$ and $CO_3^{\bullet-}$ exhibited a positive correlation with increasing Fe(III) concentrations (Fig. 5e). Notably, $^{\bullet}OH$ generation displayed pH-dependent behavior: Its concentration initially rose with pH (3.0–5.0), peaked at neutral conditions, and subsequently declined at alkaline pH (9.0). Conversely, $CO_3^{\bullet-}$ production intensified significantly under neutral to alkaline conditions (pH 7.0–9.0, Fig. 5f), demonstrating pH-tunable radical speciation. In addition, the steady-state concentration of $CO_3^{\bullet-}$ showed no positive correlation with that of $^{\bullet}OH$ across varying pH conditions. This finding strongly suggested that $^{\bullet}OH$ was not the exclusive precursor for $CO_3^{\bullet-}$ formation (Eqs. 8 and 9). Moreover, in the quenching experiment, the quenching effect of phenol was stronger than that of TBA, further confirming the previous inference. In the SPC system, the known sources of $CO_3^{\bullet-}$ mainly included the following two pathways (Eqs. 8–11) [8,39,40]. Further insights emerged from ^{13}C NMR analysis, which detected distinct HCO_4^- signal (Fig. S6 in Supporting information). This observation experimentally validated the hypothesized bicarbonate-activated peroxymonocarbonate (HCO_4^-) pathway (Eqs. 10 and 11) as competing route for $CO_3^{\bullet-}$ generation. Therefore, these findings elucidated how solution pH, Fe(III) dosage, SPC and OA concentration synergistically governed BPA degradation in the OA/Fe(III)/SPC system by dynamically modulating ROS distribution, which provides critical guidelines insights for optimizing ROS-mediated pollutant degradation strategies.

The degradation products and pathways of BPA in OA/Fe(III)/SPC system were investigated, 10 transformation products (TPs) were identified, TP number (No.), measured mass to charge ratio (*m/z*), and a pseudomolecular formula were summarized in Table S1 (Supporting information). BPA degradation could be divided into mineralization and polymerization processes. Based on the results

of mass spectrometry, the mineralization process of BPA mainly included hydroxylation reaction, oxidation demethylation and ring cleavage. Firstly, a hydroxyl group (-OH) added to the BPA radical cation adjacent to the phenolic ring (carbon No. 2 or 4) in oxygen-containing water or polyhydroxy systems and induced the hydroxylation of BPA [9]. Secondly, $CO_3^{\bullet-}$ was highly susceptible to attack isopropyl, extracted a hydrogen atom that triggered free radical chain oxidation in an oxygen environment, formed isopropyl modified TPs [24,41]. Finally, $CO_3^{\bullet-}$ and $^{\bullet}OH$ attacked the oxidation of adjacent -OH on aromatic rings, benzene ring cleavaged and the TP1-TP5 products formed. The oxidation process was similar to previous report [42,43]. In addition to the oxidation products, solid polymers with different degrees of polymerisation were also shown in the mass spectra (Fig. S7 in Supporting information). The *m/z* of 374.21, 462.21, 564.32, 651.41, 744.41, 837.59, 928.54 and 1020.65 corresponded to the 4–11 polymers of two polymers: phenol C_6H_5O (*m/z* 93) and benzyldiol-C_6H_4O- (*m/z* 92), respectively [44,45]. Such coupling and polymerisation reaction products were not uncommon in hydroxyl systems [44,46], however, they have been rarely reported in carbonate radical co-existence systems. To elucidate the role of $^{\bullet}OH$ in BPA polymerization, we conducted comparative analyses of reaction products with and without $^{\bullet}OH$ scavenging (Fig. S8 in Supporting information). Notably, significant polymerization products were detected in the $^{\bullet}OH$ suppressed system, demonstrating that other pathways competitively contribute to BPA polymerization.

Considering that the contribution of other ROS to the degradation of BPA was not significant, it was reasonable to speculate that $CO_3^{\bullet-}$ may be essential for its polymerisation degradation. Generally speaking, $^{\bullet}OH$ promoted BPA polymerization through hydrogen atom extraction (HAA), single electron transfer (SET), and radical adduct formation (RAF), generating phenoxyl radicals ($PhO^{\bullet}$) as key intermediates for coupling reactions (Fig. S9 in Supporting information). As a key active species in BPA degradation, $CO_3^{\bullet-}$ could easily interact with electron rich phenolic rings, led to unstable electronic configurations of aromatic rings. An electron was transferred from phenolic ring to $CO_3^{\bullet-}$, producing an aromatic radical cation [47]. This may be the key reason for the polymerization reactions promoted by $CO_3^{\bullet-}$. It was worth noting that steady-state concentrations of $CO_3^{\bullet-}$ were 2–3 folds higher than $^{\bullet}OH$ in OA/Fe(III)/SPC system. Consequently, future investigations must prioritize elucidating the polymerization and oxidation mechanisms governed by $CO_3^{\bullet-}$, particularly its capacity for direct ring activation beyond classical radical pathways. Notably, conventional separation techniques (*e.g.*, flocculation, precipitation, filtration) effectively remove organic polymers formed *via* polymerization from aqueous solutions [44]. However, certain degradation intermediates and byproducts of BPA may exhibit higher biological toxicity than the parent compound [48]. To evaluate this potential risk, we employed the Toxicity Estimation Software Tool (T.E.S.T.) to assess the developmental toxicity and bioconcentration factors of BPA transformation intermediates (Fig. S10 and Table S2 in Supporting information). The results indicated that both the developmental toxicity and bioconcentration potential of the secondary products were lower than those of BPA. Therefore, the OA/Fe(III)/SPC system presents an effective strategy for detoxifying BPA, significantly reducing the overall toxicity of the degradation products.

Notably, the introduction of organic reducing agents may lead to an increase in organic load, which was a major limitation of Fenton-like processes [14,22]. To address this, we evaluated the mineralization efficiency of organic compounds in the system by measuring the change in total organic carbon (TOC) before and after the reaction (Fig. S11 in Supporting information). In the OA/Fe(III)/SPC system, the TOC removal rate reached 37.4% when the degradation ratio of BPA was 95%, slightly higher than that in the Fe(II)/SPC system at pH 3.0 (35.1%). These results indicated that the additional organic load introduced by OA was negligible. Furthermore, the limited degree of mineralization suggested that BPA degradation likely occurred primarily through polymerization pathways.

The introduction of anions including Cl^-, SO_4^{2-} and HCO_3^- (each at 5.0 mmol/L) exerted a negligible impact on BPA degradation (Fig. S12 in Supporting information), while CO_3^{2-} inhibited BPA degradation because of the pH got raised. Additionally, BPA degradation maintained at 91%, 84% and 75% in tap water, river water, and the effluent from a wastewater treatment plant within 1 h, respectively, indicating that the OA/Fe(III)/SPC system is an effective method for removing BPA from natural water. Furthermore, the role of OA in iron utilization was systematically evaluated through cyclic experiments. The second-round degradation of BPA was still 85% in the system with single OA and SPC (without additional iron supplementation) (Fig. S12c), about 45% of BPA could be removed after four consecutive cycles, suggesting that this approach has the potential to significantly reduce iron sludge generation while maintaining satisfactory degradation performance.

This study systematically investigated the mechanisms of ROS generation and BPA degradation in the OA/Fe(III)/SPC system, with emphasis on the roles of Fe(II) and OA-Fe(III)/hydroperoxide complexes. The results demonstrated that OA synergistically enhanced the BPA degradation efficiency to 95%, far exceeding the performance of individual OA, Fe(III), or SPC systems, by accelerating the production of $CO_3^{\bullet-}$ and $^{\bullet}OH$. Two pH-dependent pathways were identified: under acidic conditions (pH 3.0–5.0), OA-Fe(III) complexes promoted ferrous iron regeneration and facilitated the activation of SPC to form highly ROS. At neutral pH (7.0), spectroscopic evidence indicated that a peroxy-bridged intermediate (OA-Fe(III)-OOH) directly decomposed into $CO_3^{\bullet-}$ and $^{\bullet}OH$. Thus, OA-Fe(III) and OA-Fe(III)-OOH complexes were identified as the key promoters of ROS generation under acidic and neutral conditions, respectively. Importantly, the redox potentials of OA-Fe(III)/Fe(II) couples shown a strong linear correlation with coordination stability constants ($R^2 = 0.9011$), indicating that selecting SMOAs with higher stability constants was more conducive to BPA degradation. These findings provide fundamental insight into the pH-specific mechanisms of ROS generation in iron-carboxylate/peroxide systems, supporting the rational design of SMOA-enhanced Fenton-like technologies for efficient pollutant removal.

Declaration of competing interest

The authors declare that they have no known competing financial interests or personal relationships that could have appeared to influence the work reported in this paper.

CRediT authorship contribution statement

Zhimin Xu: Writing – original draft, Methodology, Investigation. **Siyu He:** Resources, Project administration, Methodology. **Lingzhi Wang:** Resources, Project administration, Methodology. **Lei Wen:** Resources, Project administration, Methodology. **Fangfang Li:** Writing – review & editing, Formal analysis. **Hongbo Peng:** Writing – original draft, Supervision, Project administration, Methodology. **Siyao Wang:** Writing – review & editing, Formal analysis. **Kexin Chang:** Writing – review & editing, Formal analysis. **Bo Pan:** Writing – review & editing, Formal analysis. **Peng Gao:** Writing – review & editing, Supervision, Project administration, Methodology.

Acknowledgments

This research was supported by the National Nature Science Foundation of China (No. 42573059), Yunnan Talent Support Plan

Projects (No. KKXX202423042), Yunnan Fundamental Research Projects (No. 202401AT070386), Recruitment Program of Highly-Qualified Scholars in Kunming University of Science & Technology (No. KKKP201823026), Yunnan Fundamental Research Projects (No. 202501CF070165).

Supplementary materials

Supplementary material associated with this article can be found, in the online version, at doi:10.1016/j.cclet.2025.112343.

References

[1] S. Kim, C.M. Park, A. Jang, et al., J. Membr. Sci. 570-571 (2019) 77–84.
[2] Z. Luo, Y. Tu, H. Li, et al., Ecotoxicol. Environ. Saf. 167 (2019) 476–484.
[3] W. Song, J. Li, Z. Wang, et al., Sci. Total. Environ. 699 (2020) 134258.
[4] R. Mahdavi, S.S. Ashraf Talesh, Ultrason. Sonochem. 51 (2019) 230–240.
[5] J.L. Wilkinson, P.S. Hooda, J. Barker, et al., Crit. Rev. Environ. Sci. Technol. 46 (2016) 336–381.
[6] S. Yue, Z. Zhao, M. Yang, et al., Chin. Chem. Lett. 37 (2026) 112108.
[7] J. Ma, X. Xia, Y. Ma, et al., Chemosphere 205 (2018) 41–44.
[8] Y. Li, H. Dong, J. Xiao, et al., J. Hazard. Mater. 442 (2023) 130014.
[9] J. Gao, X. Duan, K. O'Shea, D.D. Dionysiou, Water Res. 171 (2020) 115394.
[10] H. Liu, M. Cheng, Y. Liu, et al., Sep. Purif. Technol. 355 (2025) 129659.
[11] R. Wang, Q. Shi, W. Wang, et al., Environ. Sci.: Nano 12 (2025) 2407–2420.
[12] F.X. Dong, L. Yan, S.T. Huang, et al., Process. Saf. Environ. Prot. 157 (2022) 411–419.
[13] H. Lv, Y. Huo, M. Cheng, et al., Chemosphere 335 (2023) 139020.
[14] Z. Yang, C. Shan, B. Pan, J.J. Pignatello, Environ. Sci. Technol. 55 (2021) 8299–8308.
[15] Y. Zhang, M. Zhou, J. Hazard. Mater. 362 (2019) 436–450.
[16] X. Jin, Y. Wang, Y. Huang, et al., Chin. Chem. Lett. 35 (2024) 109499.
[17] Y. Wang, D. Huang, C. Ge, et al., J. Hazard. Mater. 457 (2023) 131799.
[18] J. Huang, A. Jones, T.D. Waite, et al., Chem. Rev. 121 (2021) 8161–8233.
[19] T. Pan, Y. Wang, X. Yang, et al., Chem. Eng. J. 384 (2020) 123248.
[20] S. Yang, Z.H. Liang, Y. Wen, et al., ACS EST Eng. 3 (2023) 271–282.
[21] S. Li, J. Zou, J. Wu, et al., Water Res. 259 (2024) 121891.
[22] Z. Yang, Y. Cui, B. Pan, J.J. Pignatello, Environ. Sci. Technol. 57 (2023) 18918–18928.
[23] L. Lespade, Comput. Theor. Chem. 1135 (2018) 6–10.
[24] Z. Hao, J. Ma, C. Miao, et al., Environ. Sci. Technol. 54 (2020) 10118–10127.
[25] L. Lian, B. Yao, S. Hou, et al., Environ. Sci. Technol. 51 (2017) 2954–2962.
[26] W. Ren, C. Cheng, P. Shao, et al., Environ. Sci. Technol. 56 (2021) 78–97.
[27] Z. Xu, Z. Liu, S. Li, et al., J. Environ. Manage. 354 (2024) 120211.
[28] Q. Zhou, W. Niu, Y. Li, X. Li, J. Clean. Prod. 258 (2020) 120790.
[29] J. Qu, X. Tian, X. Zhang, et al., Appl. Catal. B: Environ. 310 (2022) 121359.
[30] C.M. Hendy, G.C. Smith, Z. Xu, et al., J. Am. Chem. Soc. 143 (2021) 8987–8992.
[31] S. Chen, Y. Xiang, Q. Yang, et al., Chin. Chem. Lett. 37 (2026) 111838.
[32] L. Guo, Z. Nie, L. Wen, et al., Sci. Total. Environ. 902 (2023) 165883.
[33] Y. Zhou, X. Fang, T. Wang, et al., Chem. Eng. J. 313 (2017) 638–645.
[34] P. Salgado, V. Melin, M. Albornoz, et al., Appl. Catal. B: Environ. 226 (2018) 93–102.
[35] T.J. Strathmann, A.T. Stone, Environ. Sci. Technol. 36 (2002) 5172–5183.
[36] C. Chen, Y. Wang, Y. Huang, et al., Appl. Catal. B: Environ. 321 (2023) 122062.
[37] Y. Pan, R. Qin, M. Hou, et al., Sep. Purif. Technol. 300 (2022) 121831.
[38] S. Meng, P. Zhou, Y. Sun, et al., Water Res. 218 (2022) 118412.
[39] B.T. Zhang, Z. Yan, J. Zhao, et al., Water Res. 243 (2023) 120340.
[40] H. Yang, J. Liu, B.T. Zhang, et al., Appl. Catal. B: Environ. 377 (2025) 125483.
[41] J. Gao, R.F. Nunes, K. O'Shea, et al., Water Res. 219 (2022) 118457.
[42] C.M. Liu, Z.H. Diao, W.Y. Huo, et al., Environ. Pollut. 239 (2018) 698–705.
[43] Z.H. Diao, F.X. Dong, L. Yan, et al., J. Hazard. Mater. 384 (2020) 121385.
[44] Y. Chen, W. Ren, T. Ma, et al., Environ. Sci. Technol. 58 (2024) 4844–4851.
[45] J. Dou, Y. Tang, Z. Lu, et al., Environ. Sci. Technol. 57 (2023) 5703–5713.
[46] Z. Wang, W. Qiu, S.Y. Pang, et al., Environ. Sci. Technol. 56 (2022) 1492–1509.
[47] J.S. Moore, G.O. Phillips, A. Sosnowski, Int. J. Radiat. Biol. Relat. Stud. Phys. Chem. Med. 31 (1977) 603–605.
[48] M.S. Rahman, E.O. Adegoke, M.G. Pang, J. Hazard. Mater. 417 (2021) 126076.